



Universiteit
Leiden

The Netherlands

Reactivity of cobalt(II)-dichalcogenide complexes: correlation between redox conversion and ligand-field strength

Marvelous, C.

Citation

Marvelous, C. (2022, July 5). *Reactivity of cobalt(II)-dichalcogenide complexes: correlation between redox conversion and ligand-field strength*. Retrieved from <https://hdl.handle.net/1887/3421554>

Version: Publisher's Version

License: [Licence agreement concerning inclusion of doctoral thesis in the Institutional Repository of the University of Leiden](#)

Downloaded from: <https://hdl.handle.net/1887/3421554>

Note: To cite this publication please use the final published version (if applicable).

Chapter 5

Structural Investigations and Reactivity of Cobalt(II)-Disulfide Complexes

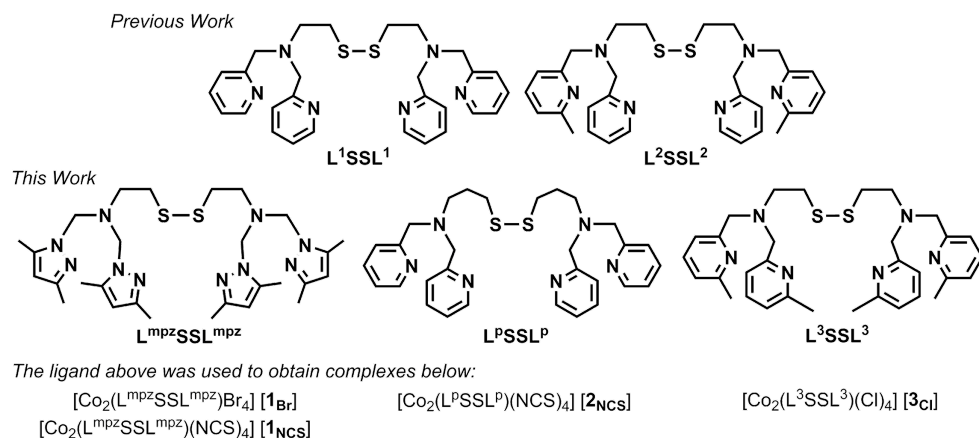
*Controlling the bio-inspired redox interconversion of Co(II)-disulfide compounds and their related Co(III)-thiolate complexes is a perplexing task as the factors triggering this reaction are not fully understood. Three disulfide ligands 2,2'-disulfanediybis(N,N-bis((3,5-dimethyl-1H-pyrazol-1-yl)methyl)ethan-1-amine) ($L^{mpz}SSL^{mpz}$), 3,3'-disulfanediybis(N,N-bis(pyridin-2-ylmethyl)propan-1-amine) (L^PSSL^P), and 2,2'-disulfanediybis(N,N-bis(6-methylpyridin-2-ylmethyl)ethan-1-amine) (L^3SSL^3) with different chain lengths and pyrazole or pyridine groups were reacted with cobalt(II) salts and the resulting complexes were studied for their potential to form Co(III)-thiolate complexes. Crystal structures of $[Co_2(L^{mpz}SSL^{mpz})(Br)_4]$ [**1Br**], $[Co_2(L^{mpz}SSL^{mpz})(NCS)_4]$ [**1Ncs**], $[Co_2(L^PSSL^P)(NCS)_4]$ [**2Ncs**], and $[Co_2(L^3SSL^3)(Cl)_4]$ [**3Cl**] show that generally the disulfide sulfur donors do not coordinate to the cobalt(II) centers, resulting in dinuclear structures containing two 5-coordinate cobalt centers. However, a unique asymmetric dinuclear complex is found in [**1Br**] in which one of the sulfur atoms coordinates to one of the cobalt ions. Thiocyanate-induced Co(III)-thiolate formation in the presence of either ligand $L^{mpz}SSL^{mpz}$ or L^PSSL^P is evidently unsuccessful, as Co(II)-disulfide complexes were obtained. The reaction of all Co(II)-disulfide complexes with 8-quinolinol suggest that redox conversion to Co(III)-thiolate complexes may take place, but the reactions are not clean.*

This chapter will be submitted for publication: Christian Marvelous, Maxime A. Siegler, and Elisabeth Bouwman, *manuscript in preparation*

5.1. Introduction

The conversion of specific metal⁽ⁿ⁾-disulfide complexes into the corresponding redox-interconverted metal⁽ⁿ⁺¹⁾-thiolate complexes has emerged recently as an interesting field of study. The study of this redox-conversion reaction is inspired by the natural enzymes, in which the thiol/disulfide conversion and redox reactions are important in for example glutaredoxins, thioredoxins, or in the heme binding of the heme oxygenase enzyme.¹⁻⁴ In the past two decades, several examples of the redox conversion of copper(I)-disulfide complexes into the corresponding copper(II)-thiolate complexes have been reported. The ligand structures were shown to have a large influence on the formation of either a dinuclear *transoid*-Cu(I)-disulfide, *cisoid*-Cu(I)-disulfide, or Cu(II)- μ -thiolate complex.^{5,6}

Recently, the study of redox interconversion reactions has progressed from copper to cobalt complexes. The ligand L¹SSL¹ (**Scheme 5.1**) used in the formation of Cu(II)- μ -thiolate complex was shown to form dinuclear Co(II)-disulfide complexes when reacted with cobalt(II) halides; however, the reaction with cobalt(II) thiocyanate resulted in the corresponding Co(III)-thiolate compound.⁷ On the other hand, the slightly different ligand L²SSL² (**Scheme 5.1**) in combination with cobalt(II) thiocyanate affords the dinuclear Co(II)-disulfide complex instead of a Co(III)-thiolate complex.⁸ These studies show that the changes in the disulfide ligand structure have a large effect on the formation of either Co(II)-disulfide complex or Co(III)-thiolate complex. However, the delicate balance between



Scheme 5.1. Various ligand structures reported in previous work and in the present work, along with the formula of the complexes obtained using the ligand in the present work.

Co(II)-disulfide and Co(III)-thiolate complexes has been shown to be also sensitive to alteration of the coordination environment such as addition or removal of halides, change in solvents, or the addition of external ligands.⁷⁻¹⁰

The occurrence of finite examples of Co(II)-disulfide to Co(III)-thiolate redox conversion limits our current understanding of the factors triggering these reactions. Thus, the difference in reactivity of various disulfide ligands with Co(II) salts is a point of interest for additional studies. Therefore, in the research described in this Chapter, the three ligands depicted in **Scheme 5.1** were reacted with different Co(II) salts to see whether Co(III)-thiolate complexes could be formed. The ligand $L^{\text{mpz}}\text{SSL}^{\text{mpz}}$ was previously used in reactions with Cu(I) and Cu(II) salts and resulted in the formation of Cu(I)-disulfide and Cu(II)-disulfide complexes.¹¹ Also for $L^3\text{SSL}^3$, reaction with a Cu(I) salt resulted in formation of the Cu(I)-disulfide.⁵ The ligand $L^{\text{p}}\text{SSL}^{\text{p}}$ is new; its structure is similar to that of $L^1\text{SSL}^1$, the only difference being propylene instead of an ethylene bridges between the disulfide moiety and the tertiary amines on the structure. Therefore, the change in the electronic effect of the ligand $L^{\text{p}}\text{SSL}^{\text{p}}$ compared to the ligand $L^1\text{SSL}^1$ is minimal and its reactivity to form a Co(III)-thiolate complex is expected to be similar.

5.2. Results

5.2.1. Synthesis and Characterization of the Compounds

The ligands $L^{\text{mpz}}\text{SSL}^{\text{mpz}}$ and $L^3\text{SSL}^3$ were prepared following reported procedures.^{5, 11} For the ligand $L^{\text{p}}\text{SSL}^{\text{p}}$, the precursor bis(3-aminopropyl)disulfide was prepared following a literature procedure,¹² and was obtained as slightly yellow oil in 90% yield. The oil was pure enough for further reaction as characterized with ESI-MS and ¹H-NMR spectroscopy (Figure AIV.1–AIV.2). The oil was used for the preparation of $L^{\text{p}}\text{SSL}^{\text{p}}$, which was obtained as a dark brown oil in 65% yield, was characterized with ESI-MS, ¹H-NMR, and ¹³C-NMR spectroscopy (Figure AIV.3–AIV.5), and was determined to be pure enough for use in complex synthesis. The oil is stable in air for several months, although the color darkens overtime.

Addition of one equivalent of a disulfide ligand to two equivalents of a cobalt salt resulted in 69–94% yields of the cobalt(II)-disulfide complexes $[\text{Co}_2(L^{\text{mpz}}\text{SSL}^{\text{mpz}})(\text{Br})_4]$ [**1Br**], $[\text{Co}_2(L^{\text{mpz}}\text{SSL}^{\text{mpz}})(\text{NCS})_4]$ [**1Ncs**], $[\text{Co}_2(L^{\text{p}}\text{SSL}^{\text{p}})(\text{NCS})_4]$ [**2Ncs**], and $[\text{Co}_2(L^3\text{SSL}^3)\text{Cl}_4]$ [**3Cl**].

The ESI-MS spectrum of an acetonitrile solution of [**1_{Br}**] (Figure AIV.6), shows peaks that can be assigned to the species [**1_{Br}** - 2Br⁻ + HCOO⁻]⁺ at *m/z* 907.0 and [**1_{Br}** - 3Br⁻ + HCOO⁻]²⁺ at *m/z* 414.1. The ESI-MS spectrum of [**1_{NCS}**] dissolved in acetonitrile (Figure AIV.7) shows peaks at *m/z* 922.1, 760.1, and 351.2 assigned to the species [**1_{NCS}** - NCS⁻ + HCOO⁻ + H⁺]⁺, and both partially reduced species [**1_{NCS}** - 3NCS⁻]⁺ and [**1_{NCS}** - 4SCN⁻]²⁺. The ESI-MS spectrum of an acetonitrile solution of [**2_{NCS}**] (Figure AIV.9) show peaks corresponding to the species [**2_{NCS}** - NCS⁻]⁺ at *m/z* 836.0, and [**2_{NCS}** - 2NCS⁻]²⁺ at *m/z* 389.1. In the ESI-MS spectrum of an acetonitrile solution of [**3_{Cl}**] (Figure AIV.11) peaks are present for [**3_{Cl}** - 2Cl⁻ + HCOO⁻]⁺, [**3_{Cl}** - 3Cl⁻ + HCOO⁻]²⁺, and [**3_{Cl}** - 2Cl⁻]²⁺ at *m/z* 805.1, 385.1, and 380.1, respectively. Solid-state magnetic susceptibility measurements for all compounds were determined using a magnetic susceptibility balance. The values of the magnetic moment calculated for two cobalt centers in [**1_{Br}**], [**1_{NCS}**], [**2_{NCS}**], and [**3_{Cl}**] are 5.93 μ_B, 5.29 μ_B, 5.43 μ_B, and 6.19 μ_B, respectively, in agreement with the presence of two high-spin cobalt(II) centers in each of the compounds.¹³⁻¹⁵ Furthermore, ¹H-NMR spectra of [**1_{NCS}**], [**2_{NCS}**], and [**3_{Cl}**] (Figure AIV.8, AIV.10, and AIV.12) show large upfield and downfield shifts of the peaks, ranging from -57 ppm up to 83 ppm. All compounds were found to be analytically pure based on elemental analysis.

Compound [**1_{Br}**] has very limited solubility in various organic solvents, its ¹H-NMR spectrum and absorption spectrum in solution could not be obtained. In DMSO the compound is moderately soluble, however, over a short period of time the blue solution turned into pink, indicating degradation of the complex. Therefore, solid-state reflectance spectrum of the blue powder of [**1_{Br}**] (Figure AIV.13) was obtained. It shows two relatively strong peaks at 441 and 738 nm, assigned to *d-d* transitions of the cobalt(II) centers. The UV-visible absorption spectra of a dark purple solution of [**1_{NCS}**] in acetone (Figure AIV.14), bright blue-purple acetone solution of [**2_{NCS}**] (Figure AIV.15), as well as pale purple acetonitrile solution of [**3_{Cl}**] (Figure AIV.16) generally show two peaks (**Table 5.1**), that are ascribed to the *d-d* transitions of Co(II) ions in a trigonal-bipyramidal geometry.^{16, 17}

Table 5.1. UV-visible absorption of the cobalt complexes described in this work.

Compound	Absorption λ_{\max} in nm (ϵ in $M^{-1} \text{ cm}^{-1}$)
[1Br]	441 (*), 738 (*)
[1NCS]	588 (7.4×10^2) 824 (< 100)
[2NCS]	520 (3.5×10^2) 615 (4.3×10^2)
[3Cl]	545 (1.5×10^2) 588 (1.4×10^2)

* Solid state spectrum

5.2.2. Description of the Crystal Structures

Projections of the crystal structures are shown in **Figure 5.1**, selected bond distances are provided in **Table 5.2**. The crystallographic data and the complete list of bond distances and bond angles are provided in Table AIV.1–AIV.6. Compound [1Br] crystallizes in the triclinic space group $P-1$. The asymmetric unit contains one molecule of [1Br]. One of two cobalt centers in [1Br] is in a distorted trigonal-bipyramidal geometry (Co2, $\tau_5 = 0.74$),¹⁸ and the other in a slightly distorted octahedral geometry (Co1). Two bromide ions and three nitrogen atoms from the ligand $L^{\text{mpz}}\text{SSL}^{\text{mpz}}$ are coordinated to each of the cobalt centers. One of the

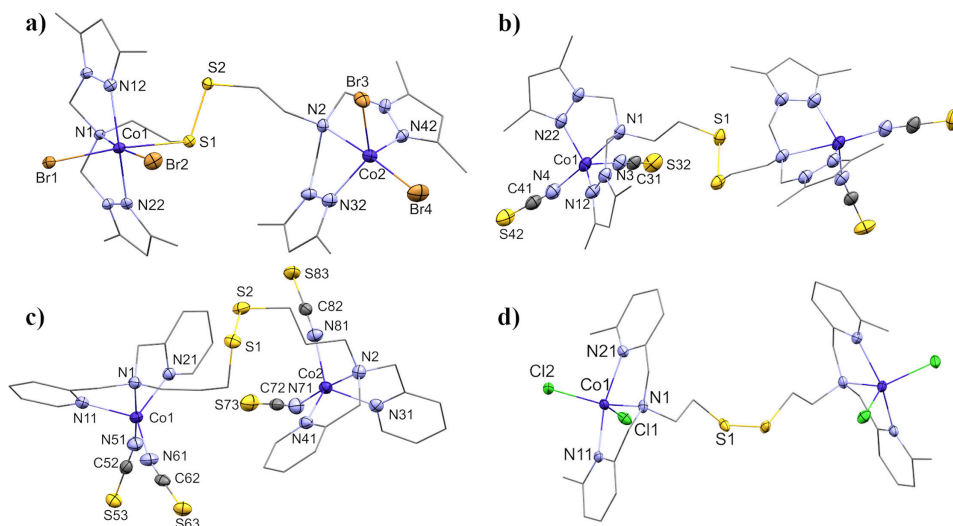


Figure 5.1. Projections of the structures of a) [1Br], b) [1NCS], c) [2NCS], d) [3Cl]. Displacement ellipsoids (50% probability) for all non-carbon atoms. Carbon atoms except those in NCS^- are shown as wireframe, and disordered moieties, hydrogen atoms and lattice solvent molecules are omitted for clarity.

Table 5.2. Selected bond distances in [1NCS], [1Br], [2NCS], and [3Cl].

Atoms	Bond distances (Å)		Atoms	Bond distances (Å)	
	[1Br]	[1NCS]		[2NCS]	[3Cl]
S1–S2	2.0454(14)	2.0396(10)	S1–S2	2.0272(9)	2.0311(12)
Co1–N1	2.264(3)	2.3701(17)	Co1–N1	2.2785(19)	2.1406(14)
Co2–N2	2.378(4)		Co2–N2	2.2337(19)	
Co1–N12	2.129(3)	2.0444(17)	Co1–N11	2.0661(19)	2.1631(14)
Co1–N22	2.060(4)	2.0400(17)	Co1–N21	2.0530(19)	2.1918(15)
Co2–N32	2.072(4)		Co2–N31	2.032(2)	
Co2–N42	2.060(4)		Co2–N41	2.0509(19)	
Co1–S1	2.6084(12)	6.0600(7)	Co1–S1	6.2951(7)	4.8457(9)
Co2–S2	6.090(1)		Co2–S2	5.6117(8)	

sulfur atoms of $L^{\text{mpz}}\text{SSL}^{\text{mpz}}$ (S1) is coordinated to Co1, completing the octahedral geometry, with the three nitrogen donor atoms bound in a meridional fashion. The asymmetric structure of [1Br] is similar to the structures of $[\text{Fe}_2(L^1\text{SSL}^1)\text{Cl}_4]$ and $[\text{Cu}_2(L^{\text{mpz}}\text{SSL}^{\text{mpz}})(\text{CH}_3\text{CN})_2(\text{BF}_4)_2]_n(\text{BF}_4)_{2n}$.^{7, 11} The distance between the coordinated sulfur donor to the cobalt(II) center is 2.6084(12) Å, which is slightly shorter than the Fe–S bond in $[\text{Fe}_2(L^1\text{SSL}^1)\text{Cl}_4]$ (2.6925(8) Å) or the Cu–S bond in $[\text{Cu}_2(L^{\text{mpz}}\text{SSL}^{\text{mpz}})(\text{CH}_3\text{CN})_2(\text{BF}_4)_2]_n(\text{BF}_4)_{2n}$ (2.7761(8) Å).^{7, 11} As a consequence of the binding of the sulfur donor atom to Co1, the Co1–N_(pyrazole) bonds are longer than the Co2–N_(pyrazole) bonds.

Compound [1NCS] crystallizes in the monoclinic space group $C2/c$. The asymmetric unit contains one half a molecule of [1NCS] (the other half of the dinuclear compound is generated by a two-fold rotation axis perpendicular to the S–S bond and one co-crystallized lattice acetonitrile molecule. The cobalt centers are in slightly distorted trigonal-bipyramidal geometries ($\tau_5 = 0.91$),¹⁸ coordinated with five nitrogen atoms, two of which are from the NCS^- ions and three from the $L^{\text{mpz}}\text{SSL}^{\text{mpz}}$ ligand. As the disulfide atoms are not coordinated to the metal centers, the S1–S2 bond is slightly shorter in [1NCS] than in [1Br].

The asymmetric unit of [2NCS] (monoclinic space group $P2_1/c$) contains one molecule of the dinuclear compound. Both cobalt centers are in a distorted trigonal-bipyramidal geometry ($\tau_5 = 0.73$ and 0.78).¹⁸ The coordination sphere of the cobalt centers is similar to those in [1NCS], comprising two nitrogen atoms from NCS^- ions and three nitrogen atoms from the ligand $L^{\text{P}}\text{SSL}^{\text{P}}$. Interestingly, the S1–S2 bond distance in [2NCS] is the shortest among all reported compounds in this manuscript. All other bond distances are similar to those in

reported cobalt(II)-disulfide complexes.⁷⁻⁹ Short contacts and stacking interactions are present between pyridine moieties of neighboring molecules, with distances ranging from 3.392 Å to 3.681 Å. The π - π -stacking interactions are in the parallel displaced conformation, as usually found for interactions between pyridine rings.¹⁹

Compound [3Cl] crystallizes in the monoclinic space group *I2/a*. The asymmetric unit contains one half of the dinuclear molecule (the other half is symmetrically generated *via* a twofold axis perpendicular to the S-S bond) and one lattice acetonitrile solvent molecule. The $-(\text{CH}_2)_2\text{-S-S-(CH}_2)_2-$ is found to be disordered over three orientations, and the occupancy factors for each component of the disorder refines to 0.7596(18), 0.110(2) and 0.131(3). Two chloride ions and three nitrogen atoms of the ligand L^3SSL^3 are coordinated to a cobalt center in a geometry that is in between trigonal bipyramid and a square pyramid. ($\tau_5 = 0.56$).¹⁸ In contrast to the other structures, where the apical positions of the trigonal bipyramid are occupied by the tertiary amine and a Br^- or NCS^- anion, in [3Cl] the apical positions are occupied by the pyridine nitrogen atoms. As a consequence, the bond distance of Co-N (tertiary amine) is shorter (2.1406(14) Å) in compound [3Cl] than in the unmethylated compound $[\text{Co}_2(\text{L}^1\text{SSL}^1)(\text{X})_4]$.^{7, 10} The presence of the methyl groups on the pyridine rings causes longer Co-N(py) distances (2.1631(14) Å and 2.1918(15) Å). Longer Co-N(py) bond distances are also observed in compounds with the ligand L^2SSL^2 (asymmetric methylated ligand) described in Chapter 3.²⁰ The presence of the methyl groups also causes the ligand L^3SSL^3 to bind in meridional fashion. The N(py)-Co-N(py) angle is 157.28°, which is significantly larger than those found on non-methylated pyridine compounds $[\text{Co}_2(\text{L}^1\text{SSL}^1)(\text{X})_4]$ (about 116°–118°).

5.2.3. Reactivity of Disulfide Complexes with Exogenous Ligand 8-quinolinolate

As described in Chapters 2 and 3, several attempts have been undertaken to generate cobalt(III)-thiolate complexes by using various exogenous ligands.^{10, 20} It was found that the anionic ligand 8-quinolinolate (quin^-) is superior in this reaction than 2,2'-bipyridine or 1,10-phenanthroline, as the use of quin^- generally leads to much cleaner reactions.²⁰ For that reason, quin^- was utilized in attempts to convert cobalt(II)-disulfide complexes of the ligands $\text{L}^{\text{mpz}}\text{SSL}^{\text{mpz}}$, $\text{L}^{\text{p}}\text{SSL}^{\text{p}}$, and L^3SSL^3 into their corresponding cobalt(III)-thiolate complexes.

The addition of 8-quinolinol (Hquin) and K_2CO_3 , to solutions containing *in situ* formed disulfide complexes of $L^{mpz}SSL^{mpz}$, L^pSSL^p , and L^3SSL^3 resulted in distinct color changes of the solutions. Isolation of the products resulted in three different brown solids, which initially were assumed to be the compounds $[Co(L^{mpz}S)(quin)]Br$, $[Co(L^pS)(quin)]Cl$, and $[Co(L^3S)(quin)]Cl$. While the ESI-MS spectra show that the cobalt(III)-thiolate species $[Co(L^{mpz}S)(quin)]^+$ (found m/z 495.0, Figure AIV.17), $[Co(L^pS)(quin)]^+$ (found m/z 475.0, Figure AIV.18), and $[Co(L^3S)(quin)]^+$ (found m/z 489.0, Figure AIV.19) were formed, the formation of these cobalt(III)-thiolate species is not clean. In all attempts formation of at least one side product is apparent, presumably the compound $[Co(quin)_2(CH_3CN)]^+$ (found m/z 387.9). In the reaction using ligand L^3SSL^3 , the cobalt(II)-disulfide species as well as free ligand are detected in the MS (See Figure AIV.19 for more details).

Other characterization techniques, such as 1H -NMR spectroscopy in methanol- d_4 (Figure AIV.20 – AIV.22) and determination of magnetic moments with a magnetic susceptibility balance also show that the solid compounds are not pure. The calculated magnetic moments (between 3.60 and 2.76 μ_B) are not in agreement with low-spin cobalt(III)-thiolate complexes and confirm the presence of starting material and/or other type of cobalt(II) compounds.

5.3. Discussion

The different reactivity of various Co(II)-disulfide compounds is of importance, as understanding of their reactivity may provide a rationale on redox conversion reactions occurring in biology. In this Chapter it is shown that reactions of the ligands $L^{mpz}SSL^{mpz}$ and L^3SSL^3 with cobalt(II) bromide or chloride afford the expected cobalt(II)-disulfide complexes $[1_{Br}]$ and $[3_{Cl}]$. The structure of $[1_{Br}]$ is unusual, as in contrast to the expected 5-coordinate geometry of the cobalt(II) ions, one of the cobalt(II) centers is in an octahedral geometry due to coordination of one of the disulfide sulfur atoms. Similar asymmetric structures were reported for $[Fe_2(L^1SSL^1)Cl_4]$ and for the polymeric compound $[Cu_2(L^{mpz}SSL^{mpz})(CH_3CN)_2(BF_4)_2]_n(BF_4)_{2n}$.^{7, 11} So far, there are only two reports on similar asymmetric compounds with cobalt(II) centers (coordination of one of disulfide sulfur atom to one cobalt, the other sulfur atom is not coordinated to any metal), in which the Co–S bond distances are 2.262 Å and 2.272 Å.^{21, 22} Compared to those, the Co–S bond distance in compound $[1_{Br}]$ is the longest at 2.6084(12) Å and can be considered semi-coordinating.

Coordination of one of the disulfide sulfur atoms to cobalt in [**1Br**] causes the S–S bond as well as Co–N(pyrazole) bonds to be slightly elongated. The geometry of the cobalt(II) ions in [**3Cl**] is intermediate to the trigonal bipyramidal and square pyramidal geometries, featuring unusual meridional binding of the three nitrogen donors of the ligand possibly due to the steric repulsion of methylated pyridine groups of L^3SSL^3 .^{23, 24}

Reaction of cobalt(II) thiocyanate with the ligand L^1SSL^1 has been reported to result in the formation of the corresponding Co(III)-thiolate compound $[Co(L^1S)(NCS)_2]$.⁷ However, with the ligands $L^{mpz}SSL^{mpz}$ and L^PSSL^P the use of cobalt(II) thiocyanate does not afford the expected Co(III)-thiolate compounds but instead the dinuclear Co(II)-disulfide compounds [**1NCS**] and [**2NCS**] were formed, similar to the reactions with the ligand L^2SSL^2 .⁸ Based on electrochemical data, it has been suggested that the ligand $L^{mpz}SSL^{mpz}$ has a stabilizing effect on the Cu(I)-disulfide system.¹¹ The stabilization of low oxidation states by the ligand $L^{mpz}SSL^{mpz}$ seems to hamper formation of the Co(III)-thiolate complex starting from $L^{mpz}SSL^{mpz}$, even with the use of the strong ligand-field NCS^- ion. We anticipated that the reaction of the ligand L^PSSL^P with $Co(SCN)_2$ would produce a cobalt(III)-thiolate complex, as the ligand L^PSSL^P is structurally similar to ligand L^1SSL^1 . Possibly, the longer chain between the disulfide and tertiary amine on L^PSSL^P disfavors coordination of the sulfur to the cobalt center due to the formation of a six-membered chelate ring. Another explanation might be that the longer Co–S distance hampers efficient electron transfer.

Finally, we investigated the reactivity of the cobalt(II)-disulfide complexes of the ligands $L^{mpz}SSL^{mpz}$, L^PSSL^P , and L^3SSL^3 with the anionic ligand 8-quinolinol (Hquin). The strong-field ligand Hquin has been described in Chapter 3 to induce conversion of Co(II)-disulfide into Co(III)-thiolate compounds with the ligands L^1SSL^1 and L^2SSL^2 .²⁰ It was found that $quin^-$ is able to generate a Co(III)-thiolate complex with L^2SSL^2 , although L^2SSL^2 structurally and electronically hampers formation of the Co(III)-thiolate complex (compared to L^1SSL^1). The initial results seemed to indicate that Co(III)-thiolate complexes were formed of the ligands $L^{mpz}S$, L^PS , and L^3S . However, whereas ESI-MS of the products indeed showed the presence of the desired Co(III)-thiolate compounds, further analysis showed the presence of side products, presumably the complex $[Co(quin)_2(MeCN)]^+$. The formation of $[Co(quin)_2(MeCN)]^+$ is unanticipated as stoichiometric amounts of Hquin were used. Our overall results indicate that the ligands $L^{mpz}SSL^{mpz}$, L^PSSL^P , and L^3SSL^3 in

combination with Co(II) salts are less prone than L^1SSL^1 or L^2SSL^2 to result in Co(III)-thiolate complexes in our reaction conditions.

5.4. Conclusion

Four new Co(II)-disulfide complexes with the ligands $L^{mpz}SSL^{mpz}$, L^pSSL^p , and L^3SSL^3 were synthesized and characterized using various spectroscopic methods. The compound [**1Br**] has a rare asymmetric structure, which can be potentially explored further as it hints on the formation of Co–S bond. The structure of compound [**3Cl**] demonstrates how changes of ligand structure causes steric repulsion and consequently changes the binding mode of the ligand as well as the geometry of the complex. Furthermore, the ligand $L^{mpz}SSL^{mpz}$ and the new ligand L^pSSL^p in combination with Co(II) thiocyanate did not result in formation of Co(III)-thiolate compounds. Reactions of cobalt(II)-disulfide complexes of the ligands $L^{mpz}SSL^{mpz}$, L^pSSL^p , and L^3SSL^3 with the ligand 8-quinolinol were not successful. The reactions were not clean, as indicated by the formation of one or more side products. Nevertheless, as the ESI-MS of the reactions indicated the presence of the desired Co(III)-thiolate compounds, these new Co(II)-disulfide complexes may be subjected to further study towards the formation of Co(III)-thiolate complexes by inducing a larger ligand field strength with external ligands, or by manipulating the temperature / pH of the solution.

5.5. Experimental section

5.5.1. General

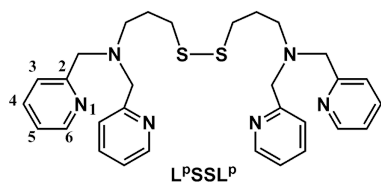
All reagents were purchased from commercial sources and used as received unless noted otherwise. Deoxygenated solvents used were obtained by the freeze-pump-thaw method followed by drying the solvents using the appropriate size of activated molecular sieves. The ligands $L^{mpz}SSL^{mpz}$ and L^3SSL^3 as well as the bis(3-aminopropyl)disulfide precursor for the ligand L^pSSL^p were prepared according to previously published procedures.^{5, 11, 12} The synthesis of the cobalt compounds was performed using standard Schlenk-line techniques under an argon atmosphere. 1H NMR spectra were recorded on a Bruker 300 DPX spectrometer at room temperature. Mass spectra were recorded on a Thermo Scientific MSQ Plus mass spectrometer with electrospray ionization (ESI) method. Formic acid was added to the eluting solvent with the final concentration of 1% (v/v). Simulated mass spectra were generated using mMass (version 5.5.0) software.²⁵ IR spectra were obtained using a PerkinElmer Spectrum Two System equipped with Universal ATR module containing

diamond crystal for single reflection (scan range 400–4000 cm^{-1} , resolution 4 cm^{-1}). Magnetic moment values were measured using a magnetic susceptibility balance (Sherwood Scientific MSB MK1) at room temperature, and the calculation of the magnetic moment follows the published procedure.²⁶ Bond distances and angles analysis of the crystal structures were performed using Mogul module on Mercury (version 4.3.1) software.²⁷ UV-visible spectra were collected using a transmission dip probe with variable path lengths and reflection probe on an Avantes AvaSpec-2048 spectrometer and using an Avalight-DH-S-Bal light source. Elemental analyses were performed by the Microanalytical Laboratory Kolbe in Germany.

5.5.2. Single crystal X-ray crystallography

All reflection intensities were measured at 110(2) K using a SuperNova diffractometer (equipped with Atlas detector) with either Mo $K\alpha$ radiation ($\lambda = 0.71073 \text{ \AA}$) for [**1Br**], [**2NCS**] and [**3Cl**] or Cu $K\alpha$ radiation ($\lambda = 1.54178 \text{ \AA}$) for [**1NCS**] under the program CrysAlisPro (Version CrysAlisPro 1.171.39.29c, Rigaku OD, 2017). The same program was used to refine the cell dimensions and for data reduction. The structure was solved with the program SHELXS-2018/3 and was refined on F^2 with SHELXL-2018/3.²⁸ Numerical absorption correction based on Gaussian integration over a multifaceted crystal model was applied using CrysAlisPro for the data of [**1Br**], [**2NCS**] and [**3Cl**]. Analytical numeric absorption correction based using a multifaceted crystal was applied using CrysAlisPro for the data of [**1NCS**]. The temperature of the data collection was controlled using the system Cryojet (manufactured by Oxford Instruments). The H atoms were placed at calculated positions using the instructions AFIX 23, AFIX 43 or AFIX 137 with isotropic displacement parameters having values 1.2 or 1.5 U_{eq} of the attached C atoms. The structures of [**1Br**] and [**2NCS**] are ordered. The structures of [**1NCS**] and [**3Cl**] are partly disordered. In the asymmetric unit [**1NCS**], one site probably contains a mixture of disordered lattice solvent molecules (MeCN and Et₂O), and that contribution has been removed from the final refinement using the SQUEEZE procedure in Platon.^{29, 30}

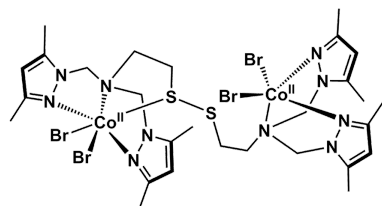
5.5.3. Synthesis of the compounds

3,3'-disulfanedylbis(*N,N*-bis(pyridin-2-ylmethyl)propan-1-amine) (L^pSSL^p)

Bis(3-aminopropyl)disulfide (1.8 grams, 10 mmol) was weighed into a clean round-bottom flask. The oil was dissolved in 150 mL methanol, after which 2-pyridinecarboxaldehyde (2.2 grams, 20 mmol, 2 equiv.) was added. The color of the solution quickly turned yellow. The pH of the solution was then adjusted to 5 by adding 37% HCl solution, and the solution was stirred overnight. Afterwards, NaCNBH₃ (1.5 grams, 23.8 mmol, 2.38 equiv.) was added in two portions. The color of the solution initially turned orange, then turned turbid to lighter yellow. The solution was stirred for another two days, then quenched by adding 37% HCl until pH 1. Methanol was removed by rotary evaporator, resulting in a yellow solution. This yellow solution was mixed with 75 mL 10 M NaOH, stirred for 30 minutes, resulting in a pale yellow solution with orange oil. The solution and oil were extracted with 3x100 mL CHCl₃. The organic layer was collected and dried over MgSO₄. The mixture was filtered and the solution was concentrated under reduced pressure to give a yellow oil. The yellow oil was redissolved in 75 mL methanol, followed by addition of 2-pyridinecarboxaldehyde (2.2 grams, 20 mmol, 2 equiv.). The pH of the solution was adjusted to 5 and the color of the solution changed to dark red. The solution was stirred for one hour. Subsequently, NaCNBH₃ (1.5 grams, 23.8 mmol, 2.38 equiv.) was added in two portions over the course of 30 minutes. The solution was stirred overnight, and subsequently quenched with 37% HCl until pH 1. The solution was then concentrated using a rotary evaporator, resulting in the formation of a red oil. The oil was treated with 75 mL NaOH 10 M and extracted with CHCl₃ (3x100mL). The organic layer was collected, dried over MgSO₄, and filtered. The solution was concentrated and a red oil was formed. The red oil was cooled in an ice bath, and dropwise addition of 10 mL 70% HClO₄ resulted in a dark brown oil. Absolute ethanol (300 mL) was added to the oil, and the mixture was stirred for 3 hours. The ethanol was decanted and the remaining oil was converted to the free base form by addition of 50 mL NaOH 10 M. The solution was again extracted with CHCl₃ (3x100mL). The organic layer was collected, dried, and filtered. Removal of the CHCl₃ under reduced pressure yielded the final product as a dark brown oil (3.5 g, 64% yield). ESI-MS found (calcd.) for [L^pSSL^p + H]⁺ *m/z* 545.2 (545.2), for

$[L^pSSL^p + 2H]^2+$ m/z 273.2 (273.1). 1H -NMR (300 MHz, CD_3CN , RT) δ (ppm): 1.75-1.84 (qu, 4H, N-CH₂-CH₂-CH₂-S), 2.52-2.62 (dt, 8H, N-CH₂-CH₂-CH₂-S), 3.73 (s, 8H, N-CH₂-Py), 7.15-7.19 (ddd, 4H, Py-H₃), 7.49-7.51 (d, 4H, Py-H₅), 7.65-7.71 (td, 4H, Py-H₄), 8.44-8.47 (m, 4H, Py-H₆). ^{13}C -NMR (75 MHz, CD_3CN , RT) δ (ppm): 26.62 (N-CH₂-CH₂-CH₂-S), 35.63 (N-CH₂-CH₂-CH₂-S), 51.93 (N-CH₂-CH₂-CH₂-S), 59.71 (N-CH₂-Py), 120.36 (Py-C₅), 124.02 (Py-C₃), 136.29 (Py-C₄), 148.81 (Py-C₆), 161.28 (Py-C₂ (quarternary carbon)).

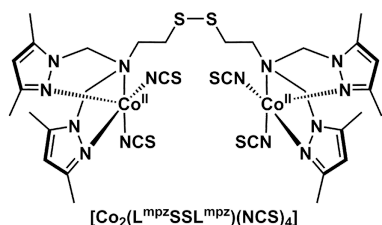
$[Co_2(L^{mpz}SSL^{mpz})(Br)_4]$ ($[1_{Br}]$)



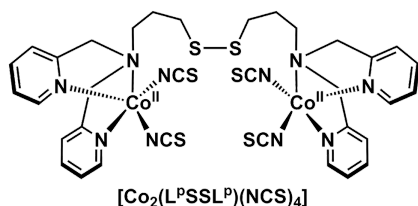
$[Co_2(L^{mpz}SSL^{mpz})(Br)_4]$

Ligand $L^{mpz}SSL^{mpz}$ (330.0 mg, 0.564 mmol) was dissolved in 5 mL dry and deoxygenated acetonitrile, resulting in a clear solution. Into the solution, solid $CoBr_2$ (249.6 mg, 1.129 mmol) was added. An intense blue solution and some blue precipitates were immediately formed, but the mixture was stirred

further for one hour. After one hour, the mixture was concentrated until approximately 1 mL was left in the flask. Into this mixture, diethyl ether was added, resulting in the formation of a blue precipitate. The precipitate was collected by filtration, washed twice with diethyl ether, dried *in vacuo*, then collected and weighed. Yield = 508.3 mg (88%) of an intense blue powder. Blue needle-shaped single crystals suitable for X-Ray diffraction were obtained using vapor diffusion of diethyl ether into a solution of $[1_{Br}]$ in methanol (although it is very poorly soluble in methanol). IR (neat, cm^{-1}): 2955w, 2921w, 1551s, 1467s, 1419s, 1386s, 1372s, 1337m, 1320m, 1300m, 1279s, 1243m, 1176w, 1147m, 1133m, 1106s, 1043s, 1015m, 982m, 948m, 905w, 863m, 825m, 812m, 800m, 783s, 762m, 717w, 688w, 662w, 633w, 626m, 613m, 597w, 581w, 555w, 521w, 491w, 471w, 451m, 406m. ESI-MS found / calcd. for $[1_{Br} - 2Br^- + HCOO^-]^+$ m/z 907.0 (907.02), for $[1_{Br} - 3Br^- + HCOO^-]^2+$ m/z 414.1 (413.5). Elemental analysis (%) for $[1_{Br}]$ ($C_{28}H_{44}Co_2S_2N_{10}Br_4$) + 0.7H₂O, calcd. C, 32.50; H, 4.42; N, 13.53; found C, 32.50; H, 4.42; N, 13.50.

[Co₂(L^{mpz}SSL^{mpz})(NCS)₄] ([1_{NCS}])

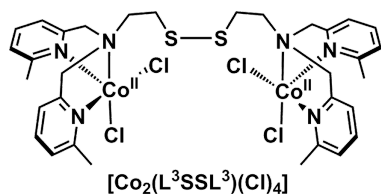
The synthesis procedure of [1_{NCS}] is similar to that of [1_{Br}], using Co(SCN)₂ instead of CoBr₂. The solution of ligand L^{mpz}SSL^{mpz} (320.0 mg, 0.547 mmol) was mixed with Co(SCN)₂ (191.6 mg, 1.094 mmol, 2 equiv.). Yield = 481.4 mg (94%). Purple single crystals suitable for X-Ray diffraction were obtained using vapor diffusion of diethyl ether into a concentrated solution of [1_{NCS}] in acetonitrile. IR (neat, cm⁻¹): 2922vw, 2059vs, 1615vw, 1550s, 1466s, 1418s, 1387s, 1335m, 1299s, 1279m, 1259m, 1242m, 1230m, 1171w, 1130m, 1104s, 1053s, 1038s, 987m, 855m, 814s, 692w, 660w, 627w, 597w, 559w, 516w, 496vw, 476m, 449w, 407vw. ESI-MS found (calcd.) for [1_{NCS} - NCS⁻ + HCOOH]⁺ *m/z* 922.1 (922.1), for [1_{NCS} - 3NCS⁻]⁺ (partial reduction from the ESI-MS) *m/z* 760.1 (760.16), and for [1_{NCS} - 4SCN⁻]²⁺ (partial reduction from the ESI-MS) *m/z* 351.09 (351.1). Elemental analysis (%) for [1_{NCS}] (C₃₂H₄₄Co₂S₆N₁₄) + 1.3H₂O, calcd. C, 40.10; H, 4.90; N, 20.46; found C, 40.05; H, 4.86; N, 20.46.

[Co₂(L^pSSL^p)(NCS)₄] ([2_{NCS}])

The dark brown oil of L^pSSL^p (54.5 mg, 0.1 mmol) was added to a Schlenk flask, followed by 5 mL dry and deoxygenated methanol to dissolve the oil. Solid Co(SCN)₂ (35.0 mg, 0.2 mmol, 2 equiv.) was added to the resulting brown solution, affording a blue-colored solution. The blue-colored solution was stirred for two hours. After two hours, the solution was concentrated until approximately 1 mL was left in the flask. Diethyl ether was added into the flask upon which a blue-purple precipitate was formed. The precipitate was filtered, washed twice with diethyl ether, followed by drying under vacuum, and weighed. Yield = 65.5 mg (73%). Dark purple single crystals suitable for X-Ray diffraction were grown using vapor diffusion of diethyl ether into the solution of [2_{NCS}] in acetonitrile. IR (neat, cm⁻¹): 2597vw, 2070vs, 2043s, 1607m, 1570w, 1479m, 1462w, 1443m, 1361w, 1286m, 1246w, 1222w, 1181w, 1156m, 1098m, 1054m, 1027m, 970w, 954m, 903w, 839w, 825w, 769s, 732m, 651m, 550w, 477m, 417m. ESI-MS found / calcd. for [2_{NCS} - NCS⁻]⁺

m/z 836.0 (836.0), for $[2\text{NCS} - 2\text{NCS}]^{2+}$ m/z 389.1 (389.0). Elemental analysis (%) for $[2\text{NCS}]$ ($\text{C}_{34}\text{H}_{36}\text{Co}_2\text{S}_6\text{N}_{10}$) + $0.5\text{C}_4\text{H}_{10}\text{O}$ (diethyl ether), calcd. C, 46.39; H, 4.43; N, 15.03; found C, 46.58; H, 4.09; N, 15.02.

$[\text{Co}_2(\text{L}^3\text{SSL}^3)(\text{Cl})_4]$ ($[\mathbf{3Cl}]$)



In a Schlenk flask, the ligand L^3SSL^3 (57.3 mg, 0.1 mmol) was dissolved in 3 mL dry and deoxygenated methanol, after which solid anhydrous CoCl_2 (25.9 mg, 0.2 mmol, 2 equiv.) was added. The purple solution was initially clear, but overtime a

precipitate formed. The solution was stirred for one hour. Concentration of the solution followed by addition of diethyl ether afforded a purple precipitate. The precipitate was filtered, washed twice with diethyl ether, then dried in vacuo and weighed. Yield = 57.1 mg (69%). Purple single crystals suitable for X-Ray diffraction were obtained using vapor diffusion of diethyl ether into the solution of $[\mathbf{3Cl}]$ in acetonitrile. IR (neat, cm^{-1}): 3674vw, 3543w, 3477w, 2987m, 2903m, 1636w, 1605s, 1575m, 1456s, 1393w, 1377m, 1346m, 1294w, 1269w, 1241w, 1221w, 1162m, 1093s, 1049m, 1011s, 963w, 909w, 896w, 874m, 792vs, 758m, 718w, 653vw, 562w, 550w, 531w, 476m, 450w, 435w, 413w. ESI-MS found (calcd.) for $[\mathbf{3Cl} - 2\text{Cl}^- + \text{HCOO}^-]^+$ m/z 805.1 (805.08), for $[\mathbf{3Cl} - 3\text{Cl}^- + \text{HCOO}^-]^{2+}$ m/z 385.1 (385.1), and for $[\mathbf{3Cl} - 2\text{Cl}^-]^{2+}$ m/z 380.1 (380.04). Elemental analysis (%) for $[\mathbf{3Cl}]$ ($\text{C}_{32}\text{H}_{40}\text{Co}_2\text{S}_2\text{N}_6\text{Cl}_4$) + $0.5\text{H}_2\text{O}$, calcd. C, 45.67; H, 4.91; N, 9.99; found C, 45.61; H, 4.78; N, 9.99.

5.5.4. Reactivity of Co(II)-disulfide complexes with 8-quinolinolol

In a typical reaction in a Schlenk flask under argon atmosphere, 0.2 mmol of ligand ($\text{L}^{\text{mpz}}\text{SSL}^{\text{mpz}}$, $\text{L}^{\text{p}}\text{SSL}^{\text{p}}$, or L^3SSL^3) was dissolved in 5 mL dry and deoxygenated methanol. To the solution, 0.4 mmol (2 equiv.) of anhydrous CoX_2 ($\text{X}=\text{Br}$ for $\text{L}^{\text{mpz}}\text{SSL}^{\text{mpz}}$, $\text{X}=\text{Cl}$ for $\text{L}^{\text{p}}\text{SSL}^{\text{p}}$ and L^3SSL^3) was added to generate the Co(II)-disulfide complexes $[\text{Co}_2(\text{L}^{\text{mpz}}\text{SSL}^{\text{mpz}})(\text{Br})_4]$ ($[\mathbf{1Br}]$), $[\text{Co}_2(\text{L}^{\text{p}}\text{SSL}^{\text{p}})(\text{Cl})_4]$ ($[\mathbf{2Cl}]$) or $[\text{Co}_2(\text{L}^3\text{SSL}^3)(\text{Cl})_4]$ ($[\mathbf{3Cl}]$). The solution was stirred for an hour at room temperature, after which 8-quinolinolol (Hquin, 0.4 mmol, 2 equiv. to the ligand) was added along with 0.4 mmol of anhydrous K_2CO_3 . In all attempts the solution turned dark brown immediately. The solution was stirred overnight under argon atmosphere,

resulting in a formation of white precipitates (presumably KX salt or unreacted K_2CO_3). The solution was filtered into a Schlenk flask under argon using a syringe filter. The filtrate was concentrated under vacuum until approximately 1 mL of solvent was left in the flask. Into this concentrated solution, 12 mL of diethyl ether was added to precipitate the complex as a brown powder. The excess of diethyl ether in the solution was removed by filtration, and the powder was washed with diethyl ether twice or until the color of the solution remained transparent. Subsequent drying of the product in vacuo afforded brown powders, which were presumed to be $[Co(L^{mpzS})(quin)]Br$, $[Co(L^pS)(quin)]Cl$, or $[Co(L^3S)(quin)]Cl$ with the yield of 159 mg, 113 mg, and 83 mg, respectively. The products were further characterized with ESI-MS, 1H -NMR spectroscopy, and with a magnetic susceptibility balance. The ESI-MS spectra and 1H -NMR spectra can be found on Appendix AIV.17 – AIV.22.

5.6. References

1. Nakamura, H., Nakamura, K. and Yodoi, J. *Annu. Rev. Immunol.* **1997**, 15, 351-369.
2. Ragsdale, S. W. and Yi, L. *Antioxid. Redox Signal.* **2011**, 14 (6), 1039-1047.
3. Wouters, M. A., Fan, S. W. and Haworth, N. L. *Antioxid. Redox Signal.* **2010**, 12 (1), 53-91.
4. Xiao, Z., La Fontaine, S., Bush, A. I. and Wedd, A. G. *J. Mol. Biol.* **2019**, 431 (2), 158-177.
5. Itoh, S., Nagagawa, M. and Fukuzumi, S. *J. Am. Chem. Soc.* **2001**, 123 (17), 4087-4088.
6. Ueno, Y., Tachi, Y. and Itoh, S. *J. Am. Chem. Soc.* **2002**, 124 (42), 12428-12429.
7. Jiang, F., Siegler, M. A., Sun, X., Jiang, L., Fonseca Guerra, C. and Bouwman, E. *Inorg. Chem.* **2018**, 57 (15), 8796-8805.
8. Jiang, F., Marvelous, C., Verschuur, A. C., Siegler, M. A., Teat, S. J. and Bouwman, E. *Inorg. Chim. Acta* **2022**, 120880.
9. Gennari, M., Gerey, B., Hall, N., Pecaut, J., Collomb, M.-N., Rouzies, M., Clerac, R., Orio, M. and Duboc, C. *Angew. Chem. Int. Ed.* **2014**, 53 (21), 5318-5321.
10. Marvelous, C., de Azevedo Santos, L., Siegler, M. A., Fonseca Guerra, C. and Bouwman, E. *Dalton Trans.* **2022**, 51, 8046-8055.
11. Ordng-Wenker, E. C. M., Siegler, M. A. and Bouwman, E. *Inorg. Chim. Acta* **2015**, 428, 193-202.
12. Doi, J. T. and Musker, W. K. *J. Org. Chem.* **2002**, 50 (1), 1-4.
13. Dori, Z. and Gray, H. B. *Inorg. Chem.* **1968**, 7 (5), 889-&.
14. Mulyana, Y., Alley, K. G., Davies, K. M., Abrahams, B. F., Moubaraki, B., Murray, K. S. and Boskovic, C. *Dalton Trans.* **2014**, 43 (6), 2499-2511.
15. Suzuki, M., Kanatomi, H. and Murase, I. *Bull. Chem. Soc. Jpn.* **1984**, 57 (1), 36-42.
16. Chan, S. L.-F., Lam, T. L., Yang, C., Lai, J., Cao, B., Zhou, Z. and Zhu, Q. *Polyhedron* **2017**, 125, 156-163.
17. Massoud, S. S., Broussard, K. T., Mautner, F. A., Vicente, R., Saha, M. K. and Bernal, I. *Inorg. Chim. Acta* **2008**, 361 (1), 123-131.
18. Addison, A. W., Rao, T. N., Reedijk, J., Vanrijn, J. and Verschoor, G. C. *J. Chem. Soc., Dalton Trans.* **1984**, (7), 1349-1356.
19. Janiak, C. *J. Chem. Soc., Dalton Trans.* **2000**, (21), 3885-3896.
20. Marvelous, C., de Azevedo Santos, L., Siegler, M. A., Fonseca Guerra, C. and Bouwman, E. **2022**, submitted
21. Lydon, J. D., Elder, R. C. and Deutsch, E. *Inorg. Chem.* **2002**, 21 (8), 3186-3197.
22. Nosco, D. L., Elder, R. C. and Deutsch, E. *Inorg. Chem.* **1980**, 19 (9), 2545-2551.

-
23. Graddon, D. P., Watton, E. C., Schulz, R. and Weeden, D. G. *Nature* **1963**, 198 (4887), 1299- &.
 24. Nagao, H., Komeda, N., Mukaida, M., Suzuki, M. and Tanaka, K. *Inorg. Chem.* **1996**, 35 (23), 6809-6815.
 25. Strohmalm, M., mMass - Open Source Mass Spectrometry Tool. www.mmass.org
 26. Bain, G. A. and Berry, J. F. *J. Chem. Educ.* **2008**, 85 (4), 532-536.
 27. Macrae, C. F., Sovago, I., Cottrell, S. J., Galek, P. T. A., McCabe, P., Pidcock, E., Platings, M., Shields, G. P., Stevens, J. S., Towler, M. and Wood, P. A. *J. Appl. Crystallogr.* **2020**, 53, 226-235.
 28. Sheldrick, G. M. *Acta Crystallogr. Sect. A: Found. Crystallogr.* **2008**, 64, 112-122.
 29. Spek, A. L. *Acta Crystallogr. Sect. C: Cryst. Struct. Commun.* **2015**, 71 (Pt 1), 9-18.
 30. Spek, A. L. *Acta Crystallogr. Sect. D. Biol. Crystallogr.* **2009**, 65 (2), 148-155.

